Nanoscale Res Lett (2007) 2:28–33
DOI 10.1007/s11671-006-9025-5

NANO EXPRESS

Transformation of β-Ni(OH)$_2$ to NiO nano-sheets via surface nanocrystalline zirconia coating: Shape and size retention

Ming-Yao Cheng · Bing-Joe Hwang

Published online: 11 November 2006

Abstract Shape and size of the synthesized NiO nano-sheets were retained during transformation of sheet-like β-Ni(OH)$_2$ to NiO at elevated temperatures via nano-sized zirconia coating on the surface of β-Ni(OH)$_2$. The average grain size was 6.42 nm after 600 °C treatment and slightly increased to 10 nm after 1000 °C treatment, showing effective sintering retardation between NiO nano-sheets. The excellent thermal stability revealed potential application at elevated temperatures, especially for high temperature catalysts and solid-state electrochemical devices.

Keywords Thermal stability · Nickel oxide · Solid oxide fuel cell · Surface coating · Anode

Introduction

Handling shapes and sizes of nanostructured materials is of great scientific interest as much of their superior properties are directly linked to high chemical or electrochemical active sites or specific nanostructures. However, it is technologically difficult to apply nanostructured materials at high temperatures since serious sintering of materials would cause loss of active sites. In order to preserve nanostructured natures of materials at elevated temperatures, retardation of sintering behaviors was considered. However, only few reports emphasized stabilization of the nanostructured materials at high temperatures [1–5]. Pang et al. showed the size of SnO_2 nanoparticles could be controlled as small as 3.5 nm even heat treatment at 600 °C [3]. Wu et al. found that surface-modified methylsiloxyl groups on the metal oxide gel could prevent grain growth of metal oxides during high temperature treatments and excellent gas sensing properties were shown [4]. Lyu et al. also showed that the thermal stabilities of mesoporous metal oxides were improved by introducing silicon-contained hybrid Gemini surfactants as a nano-propping agent [5].

Nevertheless, in electrochemical systems, dimension of three-phase-boundary (TPB) length (the region that reactants, electrode and electrolyte materials coexist) plays an important role in the corresponding performances. In solid-state electrochemical devices, such as gas sensors and solid oxide fuel cells (SOFCs), high temperature treatment could not be avoided during fabrication and operation. Consequently, surface area and TPB length are significantly decreased. Studies aiming on how to retain surface areas and microstructures of electrodes during heat treatment are highly needed [6–8]. Ozin et al. synthesized a series of mesoporous materials for SOFC electrodes [9–13] and showed better electrochemical performance on oxygen reduction [13]. However, thermal stability of the mesoporous materials needed to be further improved [9, 13]. Liu et al. have also synthesized nanostructured electrodes by a combustion CVD technique for SOFC application and the electrode material about 50 nm in grain size with higher performances were disclosed at low operating temperatures [14].

M.-Y. Cheng · B.-J. Hwang
Nano-electrochemistry Laboratory Department of Chemical Engineering, National Taiwan University of Science and Technology, Taipei 106, Taiwan, ROC

B.-J. Hwang (✉)
National Synchrotron Radiation Research Center, Hsinchu 300, Taiwan, ROC
e-mail: bjh@mail.ntust.edu.tw

Herein, we attempted to synthesize electrode materials with high thermal stability. Nickel oxide nano-sheets were coated with small zirconia clusters on the surface. Details of the nanostructure were also explored.

Experimental

The standard process for synthesizing ZrO_2-coated NiO nano-sheets was described as follows. 0.03 mol $Ni(NO_3)_2$ (Acros) was dissolved in 50 ml de-ionized water. Meanwhile, 0.12 mol NaOH (Acros) was dissolved in 50 ml de-ionized water followed by dropping in to a $Ni(NO_3)_2$ solution to form precipitates. The precipitates were filtered and washed with de-ionized water for several times and dried at 80 °C. The crystalline structure of the dried precipitates was characterized by XRD and was confirmed as hexagonal β-$Ni(OH)_2$. Then, 0.03 mol as-prepared β-$Ni(OH)_2$ was transferred into 100 ml 1-propanol (Acros) and mixed for 5 h to form a well-dispersed solution. Later, 0.001 mol zirconium-1-propoxide (70 wt% in 1-propanol, Aldrich) was added and the reactor was sealed immediately followed by stirring for 3 days. Finally, the solution was heated at 90 °C in an oil bath to remove the solvent. The obtained dried gels were transferred to furnace immediately for heating at the target temperatures (600, 700, 800, 900 and 1000 °C) with a heating rate of 5 °C/min and the holding time was 1 h. For comparison, β-$NiOH_2$ mixed with the same amount of zirconia was calcined at different temperatures.

For characterization of the synthesized samples, XRD (Rigaku D/Max-RC, Japan) with CuKα as radiation source (λ = 1.5406 A) was performed at 40 kV and 100 mA. TEM images were obtained by JSM 1010 with accelerating voltage of 80 kV. High resolution images were obtained by TECNAI F20 FEGTEM operated at the accelerating voltage of 200 kV. For TEM sample preparation, 0.01 g powder was added into 20 ml ethanol followed by ultrasonic treatment for 30 min. Later, 0.05 ml solution was dropped on to a carbon-coated Cu grid and then dried at 80 °C for TEM analysis. For nitrogen absorption analysis, the samples were heated at 250 °C in vacuum to removed absorbed water before analyzing. The surface areas were estimated according to BET equation.

Results and discussion

The basic concept for synthesis of the ZrO_2-coated NiO nano-sheets is illustrated in Fig. 1. First, β-nickel hydroxide was well dispersed in the organic solvent. Appropriate amount of zirconium n-propoxide was then added to the solution. The added zirconium n-propoxide reacted with the surface hydroxyl groups of the $Ni(OH)_2$:

$$\mathrm{Ni_{surface}} - (\mathrm{OH}) + \mathrm{Zr(OC_3H_7)_4} \rightarrow \mathrm{Ni_{surface}} - \mathrm{O} - \mathrm{Zr(OC_3H_7)_3} + \mathrm{C_3H_7OH} \quad (1)$$

In Eq. 1, $Ni_{surface}$ represents the Ni^{2+} ions on the surface of the $Ni(OH)_2$. The referred reaction was due to the strong hydrolysis nature of inorganic alkoxide with the hydroxyl groups. Then, the obtained $Ni(OH)_2$ underwent drying and heat treatment to form the NiO materials with small ZrO_2 clusters coating on the surface.

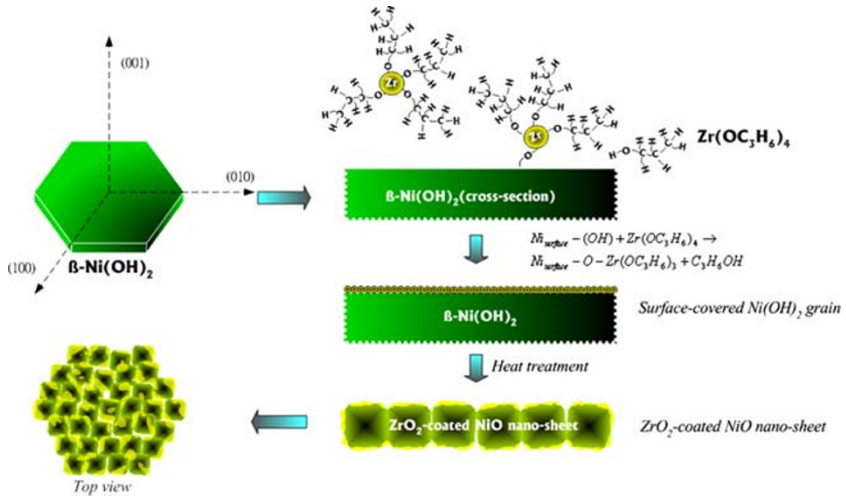

Fig. 1 Schematic illustration of synthesis of ZrO_2-coated NiO nano-sheet

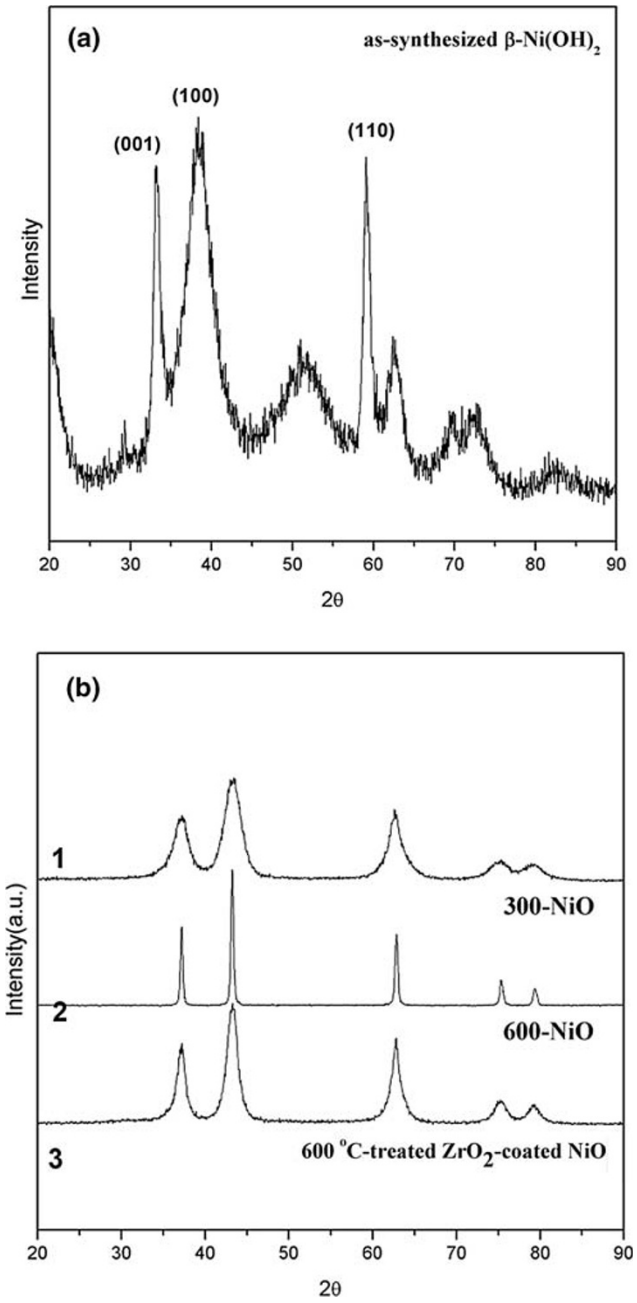

Fig. 2 XRD patterns of (**a**) the synthesized β-Ni(OH)$_2$, (**b1**) 300-NiO, (**b2**) 600-NiO, and (**b3**) 600 °C-treated ZrO_2-coated NiO

The as-synthesized Ni(OH)$_2$ precursors were first examined by XRD (Fig. 2a). From the obtained XRD pattern, it indicated the brucite-like crystalline structure of β-Ni(OH)$_2$ was obtained [15–18]. The sharp (1 0 0) and (1 1 0) peaks with the average diameters of the corresponding planes were respectively 9.23 nm and 9.84 nm by the Debye–Scherrer equation, indicating the shape of the synthesized hexagonal β-Ni(OH)$_2$ grains close to regular hexagon with almost the same dimensions of the two diagonals. Further, the average thickness of the hexagonal grains could also be estimated to be 2.65 nm according to (0 0 1) peak. The results were also confirmed with the literatures [19, 20].

The prepared Ni(OH)$_2$ precursors were first heated at 300 °C for 1 h to form NiO (denoted as 300-NiO). The XRD pattern was shown in Fig. 2(b1), indicating the formation of NiO cubic structure. By estimating the full width at half maximum (FWHM) of (2 0 0) peak, the thickness of 300-NiO was 3.95 nm. Further, the crystalline thickness estimated by (1 1 1) and (2 2 0) peaks were 4.06 and 4.74 nm, respectively. From the estimated crystalline thicknesses by different directions, the shape of the 300-NiO grain was close to spherical. However, from the TEM image of 300-NiO (Fig. 3a), tremendous amounts of sticks and platelets were observed, implying that the morphology of the synthesized β-Ni(OH)$_2$ was maintained after 300 °C treatment with the thickness and length of the sticks around 2–3 nm and 10 nm, respectively, close to that of the synthesized β-Ni(OH)$_2$. The inconsistency between XRD and TEM results suggested that the observed nano-sheets were possibly formed by stacking of NiO nano-grains. After heating the synthesized β-Ni(OH)$_2$ at 600 °C, nano-sized nature of the synthesized β-Ni(OH)$_2$ was no longer retained in the formed NiO (denoted as 600-NiO), which was first revealed by the sharp peaks in the XRD pattern shown in Fig. 2(b2). The calculated grain size according to (2 0 0) peak was around 25.41 nm, which was also evidenced by TEM image (Fig. 3b). Besides, grains of 600-NiO were cubic-like instead of nano-sheets, which was due to the sintering of the nano-sheets after 600 °C heat treatment.

On the other hand, the XRD pattern for the 600 °C-treated ZrO_2-coated NiO was shown in Fig. 2(b3). First, pure cubic NiO phase was revealed and monoclinic ZrO_2 was not observed. It was possible that the amount of the ZrO_2 was much less compared to that of NiO. The broadening of the peaks indicated small NiO grains were maintained by the surface ZrO_2. Again, according to the FWHM of (2 0 0) peak of the ZrO_2-coated NiO, the grain size was 6.42 nm. TEM images of the ZrO_2-coated NiO also showed sticks and hexagonal sheets the same as that of 300-NiO, except some small spherical grains were observed (Fig. 3c). Even after higher temperature treatment, the sticks and hexagonal sheets were still observed, excluding the thickness of the nano-sheets increased (Fig. 3d).

To clarify the nanostructure of the materials, high resolution TEM image of the 600 °C-treated ZrO_2-coated NiO was taken and analyzed. It was clearly shown that hexagonal sheet was coated by small

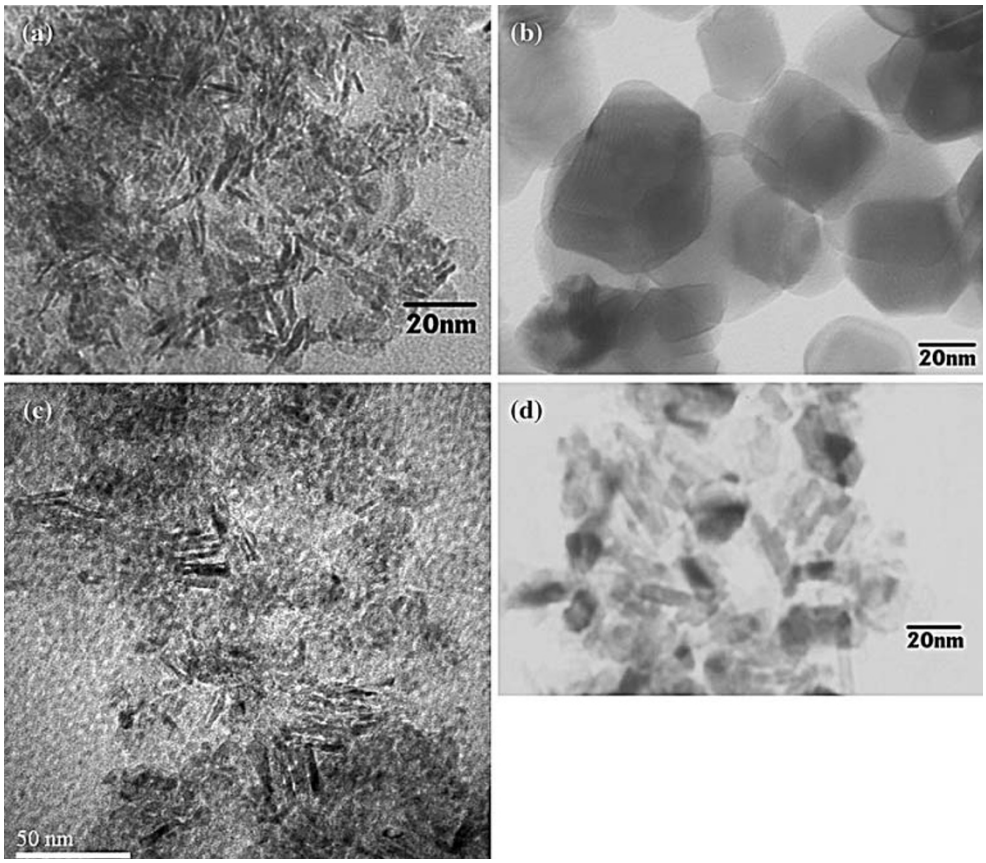

Fig. 3 TEM images of (**a**) 300-NiO, (**b**) 600-NiO, (**c**) 600 °C-treated ZrO_2-coated NiO and (**d**) 1000 °C-treated SS-NiO

spherical particles (Fig. 4a). The size of the particle was around 4–6 nm. Furthermore, the lattice image of the coated spherical particle showed the d-spacing was 0.36 nm. It indicated (0 1 1) direction of the monoclinic ZrO_2 (Fig. 4b). The d-spacing of the hexagonal sheet was 0.24 nm, which indicated (1 1 1) direction of the cubic NiO (Fig. 4c). Further analyzing the composition of spherical-particle-coated nano-sheet by EDX spectra, it revealed that the composition of the portion without spherical particles was nickel-rich (Fig. 4d) and that with spherical particles was zirconium-rich (Fig. 4e). Since the amount of ZrO_2 is only 1/30th of that of NiO (in mol), the thickness of ZrO_2 layer would be much smaller than the size of NiO nanoparticles. It is suggested that the ZrO_2 particles shown in Fig. 4a and b are exceptional, rather than typical, in size. Zirconium 1-propoxide would mainly react with the hydroxyl group on the surface of β-$Ni(OH)_2$ via hydrolysis and condensation reactions to form ZrO_2 layer. However, the ZrO_2 particles are extraordinary formed via the hydrolysis and condensation reactions of zirconium 1-propoxide in solution.

The estimated NiO grain sizes of the synthesized ZrO_2-coated NiO at different temperatures were shown in Fig. 5. It was obvious that the retention of NiO grain size was effective when comparing with that of NiO by heating physical-mixed $Ni(OH)_2$–ZrO_2. After 1000 °C treatment, the grain size of ZrO_2-coated NiO was retained around 10 nm where that of the physical-mixed NiO–ZrO_2 was larger than 50 nm. Even the sintering among the ZrO_2-coated NiO nano-sheets was still occurred, however, it was effectively retarded by the surface ZrO_2.

The fact of the nano-sized nature of the ZrO_2-coated NiO could also be evidenced by nitrogen absorption measurement. For the 600 °C-treated ZrO_2-coated NiO, the BET surface area is as high as 120.53 $m^2\ g^{-1}$ and almost seven times higher than that of the 600-NiO (17.52 $m^2\ g^{-1}$). Even after 1000 °C treatment, BET surface area of the ZrO_2-coated NiO was still as high as 42.64 $m^2\ g^{-1}$.

From the above analysis, the formation and sintering behavior of NiO were concluded. First, the hexagonal β-$Ni(OH)_2$ was treated at low temperature of 300 °C to form the hexagonal NiO nano-sheet which was stacked by NiO grains. However, the size of NiO was seriously increased and the sheet-like shape was collapsed soon after heat treatment at the temperature slightly higher than 300 °C.

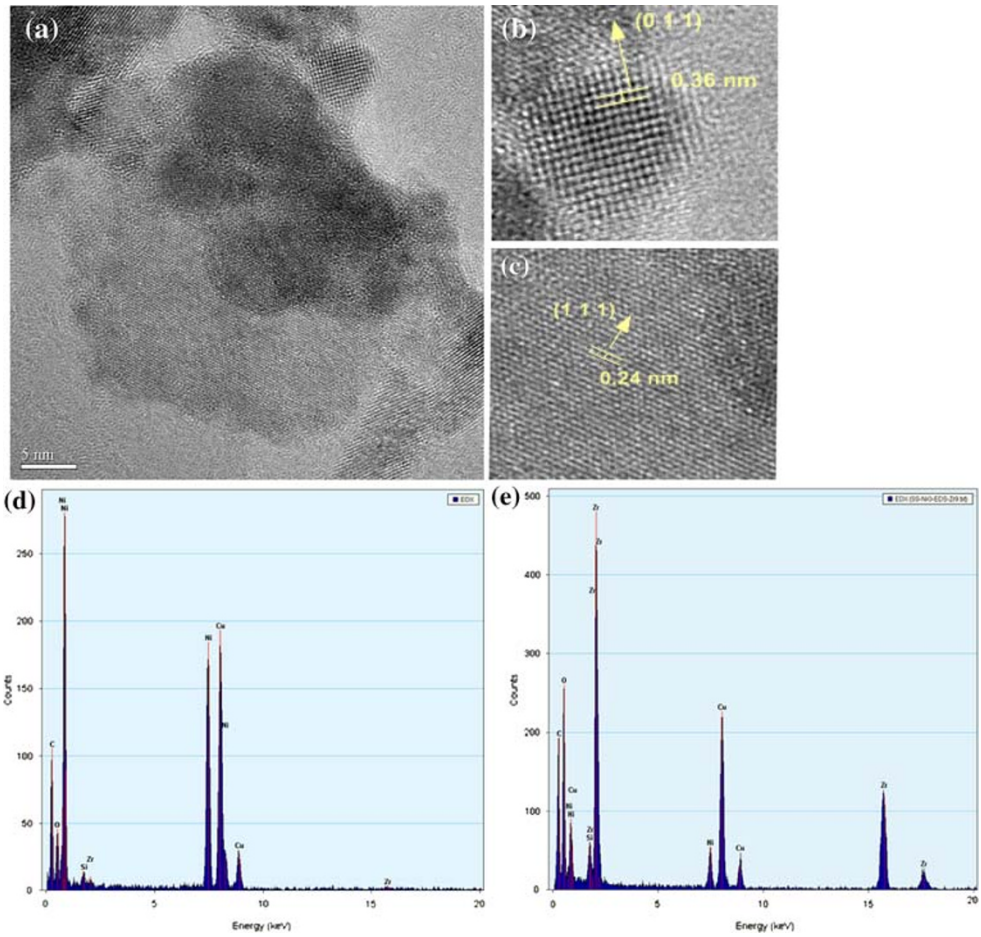

Fig. 4 (**a**) High resolution image of ZrO_2-coated NiO: (**a**) whole image, (**b**) and (**c**) are enlarging part of hexagonal nano-sheet and surface ZrO_2 particle, respectively. (**d**) and (**e**) are EDXs spectra for ZrO_2-coated NiO without and with surface ZrO_2, respectively

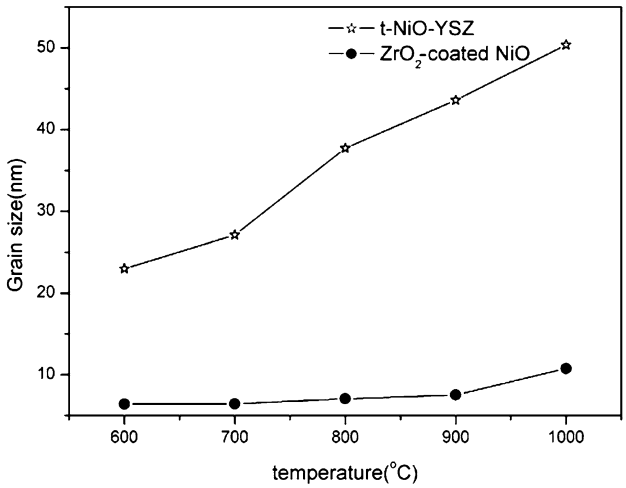

Fig. 5 Relationship of calculated grain sizes of physical mixed NiO–ZrO_2 (asterisk) and ZrO_2-coated NiO (filled circle) with temperatures

On the other hand, the ZrO_2-coated β-$Ni(OH)_2$ was also treated at temperature of 300 °C to form the ZrO_2-coated NiO. Retention of nano-sheets was clearly shown even heating at higher temperature compared to the uncoated one. The particular behavior of the synthesized ZrO_2-coated NiO nano-sheets was proposed by the surface ZrO_2 nanoparticles that limited the sintering among the NiO nano-sheets. Even after 1000 °C treatment, the shape and size of the nano-sheets were still preserved expect the slightly increase of the thickness of the nano-sheets. However, the estimated size of the NiO grains was not consistent with the size and shape observed by TEM. It was proposed to be caused by the observed nano-sheet was stacked by NiO grains.

Table 1 BET surface areas of ZrO_2-coated NiO and 600-NiO

Materials	BET surface area($m^2\ g^{-1}$)
600-NiO	17.52
600 °C-treated ZrO_2-coated NiO	120.53
800 °C-treated ZrO_2-coated NiO	85.11
1000 °C-treated ZrO_2-coated NiO	42.64

Conclusions

In this work, we have demonstrated that the retention of shape and size of β-$Ni(OH)_2$ nano-sheets during its transformation to the NiO nano-sheets was achieved by the developed method. The nanostructure was retained even after 1000 °C treatment, which was due to the existence of ZrO_2 clusters on the surface of the NiO nano-sheet. The development also opens up a new way to control the shape and size of metal oxides at high temperatures, which is a critical issue in the development of anode materials for SOFC application.

Acknowledgement The authors thank National Science Council (NSC-94-2120-M-011-002 and NSC-94-2214-E-011-010, Taiwan, R.O.C.) and National Taiwan University of Science and Technology for financial supports. FEG-TEM support from Institute of Material Science and Engineering, National Sun Yat-sen University is also acknowledged.

References

1. C. Nayral, T. Ould-Ely, A. Maisonnat, B. Chaudret, P. Fau, L. Lescouzères, A. Peyre-Lavigne, Adv. Mater. **11**, 61 (1999)
2. E.R. Leite, I.T. Weber, E. Longo, J.A. Varela, Adv. Mater. **12**, 965 (2000)
3. G. Pang, S. Chen, Y. Koltypin, A. Zaban, S. Feng, A. Gedanken, Nano. Lett. **1**, 723 (2001)
4. N.L. Wu, S.Y. Wang, I.A. Rusakova, Science **285**, 1375 (1999)
5. Y.Y. Lyu, S.H. Yi, J.K. Shon, S. Chang, L.S. Pu, S.Y. Lee, J.E. Yie, K. Char, G.D. Stucky, J.M. Kim, J. Am. Chem. Soc. **126**, 2310 (2004)
6. S.P. Jiang, Y.Y. Duan, J.G. Love, J. Electrochem. Soc. **149**, A1175 (2002)
7. E.Z. Tang, T.H. Etsell, D.G. Ivey, J. Am. Ceram. Soc. **83**, 1626 (2000)
8. U.B. Pal, S.C. Singhal, J. Electrochem. Soc. **137**, 2937 (1990)
9. M. Mamak, N. Coombs, G.A. Ozin, Adv. Funct. Mater. **11**, 59 (2001)
10. M. Mamak, N. Coombs, G.A. Ozin, Chem. Mater. **13**, 3564 (2001)
11. M. Mamak, N. Coombs, G.A. Ozin, Adv. Mater. **12**, 198 (2000)
12. M. Mamak, N. Coombs, G.A. Ozin, J. Am. Chem. Soc. **122**, 8932 (2000)
13. M. Mamak, N. Coombs, G.A. Ozin, J. Am. Chem. Soc. **125**, 5161 (2003)
14. Y. Liu, S. Zha, M. Liu, Adv. Mater. **16**, 256 (2004)
15. M. Rajamathi, P.V. Kamath, R. Seshadri, J. Mater. Chem. **10**, 503 (2000)
16. P. Jeevanandam, Y. Koltypin, A. Gedanken, Nano Lett. **1**, 263 (2001)
17. Z.H. Liang, Y.J. Zhu, X.L. Hu, J. Phys. Chem. B **108**, 3488 (2004)
18. Y.L. Lo, B.J. Hwang, Langmuir **14**, 944 (1998)
19. A.M. Fojas, E. Muphy, P. Stroeve, Ind. Eng. Chem. Res. **41**, 2662 (2002)
20. F. Bardé, M.R. Palacin, Y. Chabre, O. Isnard, J.-M. Tarascon, Chem. Mater. **16**:3936 (2004)